



# X-ray spectroscopic performance of a matrix of silicon drift diodes

Alexandre Rachevski <sup>\*1</sup>, Andrea Vacchi <sup>1</sup>, Gianluigi Zampa <sup>1</sup>, Nicola Zampa <sup>1</sup>, Irina Rashevskaya <sup>1</sup>, Andres Cicuttin <sup>2</sup>, Maria Liz Crespo <sup>2</sup>, Claudio Tuniz <sup>2</sup>



<sup>\*</sup>) corresponding author, 1) INFN - Trieste, Italy, 2) ICTP - Trieste, Italy



## ABSTRACT

Using a <sup>55</sup>Fe source we characterized the spectroscopic performance of a matrix of Silicon Drift Diodes (SDD). The matrix consists of a completely depleted volume of silicon wafer subdivided into 5 identical hexagonal cells. The back side is composed of 5 implanted arrays of increasingly negatively biased concentric p<sup>+</sup> rings. The front side, common to all 5 cells, is a shallow and uniformly implanted p<sup>+</sup> entrance window. Ionizing radiation impinging the detector bulk generates electrons that drift towards small readout n<sup>+</sup> pads placed on the back side at the center of each cell. The total sensitive area of the matrix is 135 mm<sup>2</sup>, the wafer thickness is 450 μm. We report on the layout of the experimental set-up, as well as the spectroscopic performance measured at different temperatures and bias conditions.

## 1. INTRODUCTION

SDDs [1] are successfully employed in X-ray spectroscopy due to their small readout anode geometry, which allows to minimize the serial electronic noise. In spite of this, to keep under control the parallel electronic noise component arising from the detector leakage current, SDDs have usually small dimensions (less than 1 cm<sup>2</sup>), and are normally cooled down [2, 3, 4, 5]. However, many applications (e.g. X-ray astronomy [6]) require large sensitive areas, even up to few square meters. A natural way to meet this requirement would be to design a matrix of SDDs, which exploits in the most efficient way the round shape of the silicon wafers used for the detector fabrication and, in turn, fits well to a consequent tiling in order to build up larger sensitive areas. Hexagonal shape of both the single SDD and the whole matrix would be an optimal geometry choice. The aim of this work was to characterize the spectroscopic performances of a matrix prototype made up by 5 identical hexagonal SDDs. Sections 2 and 3 describe briefly the detector and the measurement setup, while the experimental results and conclusions are presented in section 4.

## 2. THE DETECTOR

The detector is a completely depleted volume of n-type 450 μm thick silicon wafer organized as a matrix of 5 identical hexagonal SDDs. The detector total sensitive area is 135 mm<sup>2</sup>. The back side of each SDD (Fig. 1) is an arrangement of increasingly negatively biased p<sup>+</sup> rings (drift cathodes). The bias voltage of the back side is applied to the outermost drift cathode which is common to all 5 cells of the matrix. In the center of each cell there is a small n<sup>+</sup> pad (readout anode). Next to it there is the innermost drift cathode kept at a separate bias used to shield the anode from the noise of the drift cathode chain. A voltage divider integrated inside of each cell generates a potential drop between neighboring drift cathodes, thus setting up the drift field. Outside of the sensitive area of the whole matrix there are several guard rings that serve to decrease the negative bias voltage to the ground potential. The detector front side (Fig. 2), common to all 5 cells, is a shallow and uniformly implanted p<sup>+</sup> entrance window kept at a separate bias. Similar to the back side, there are several guard rings on the front side that serve to ramp down the negative bias voltage. Ionizing radiation impinging the detector bulk generates electrons that drift towards readout anodes. For the given SDD geometry the range of bias voltages that ensures effective charge collection is limited to a value that depends on silicon resistivity and wafer thickness. Figure 3 presents the readout anode leakage current of one SDD measured as a function of the back side bias voltage, whereas the front side was left floating. As the bias voltage increases the depleted volume advances from the back side towards the front side reaching it at U<sub>bias</sub> = -72 V. For larger voltages the potential of the front side p<sup>+</sup> implant follows the bias increase due to the punch-through phenomenon, and the drift channel towards the readout anode is established. The SDD continues to operate until the front side potential does not reach the punch-through threshold with the innermost drift cathode on the back side (at U<sub>bias</sub> = -160 V), and the hole current starts to flow between them. Since the innermost drift cathode is the p<sup>+</sup> ring next to the readout anode, the hole current acts as a cylindrical "curtain" where electrons drifting along the channel towards the anode recombine. Thus, the anode leakage current becomes again very small. From this simple measurement we acquire the following practical rules for the SDD correct biasing. First, the bias voltage for the front side should be high enough to deplete completely the detector volume, but it must remain lower than the punch-through threshold between the front side and the innermost drift cathode on the back side. Second, the bias voltage of the back side should not reach the punch-through threshold between the front side and the outermost drift cathode. In fact, the second rule puts the limit to the maximum drift field for a given SDD geometry.

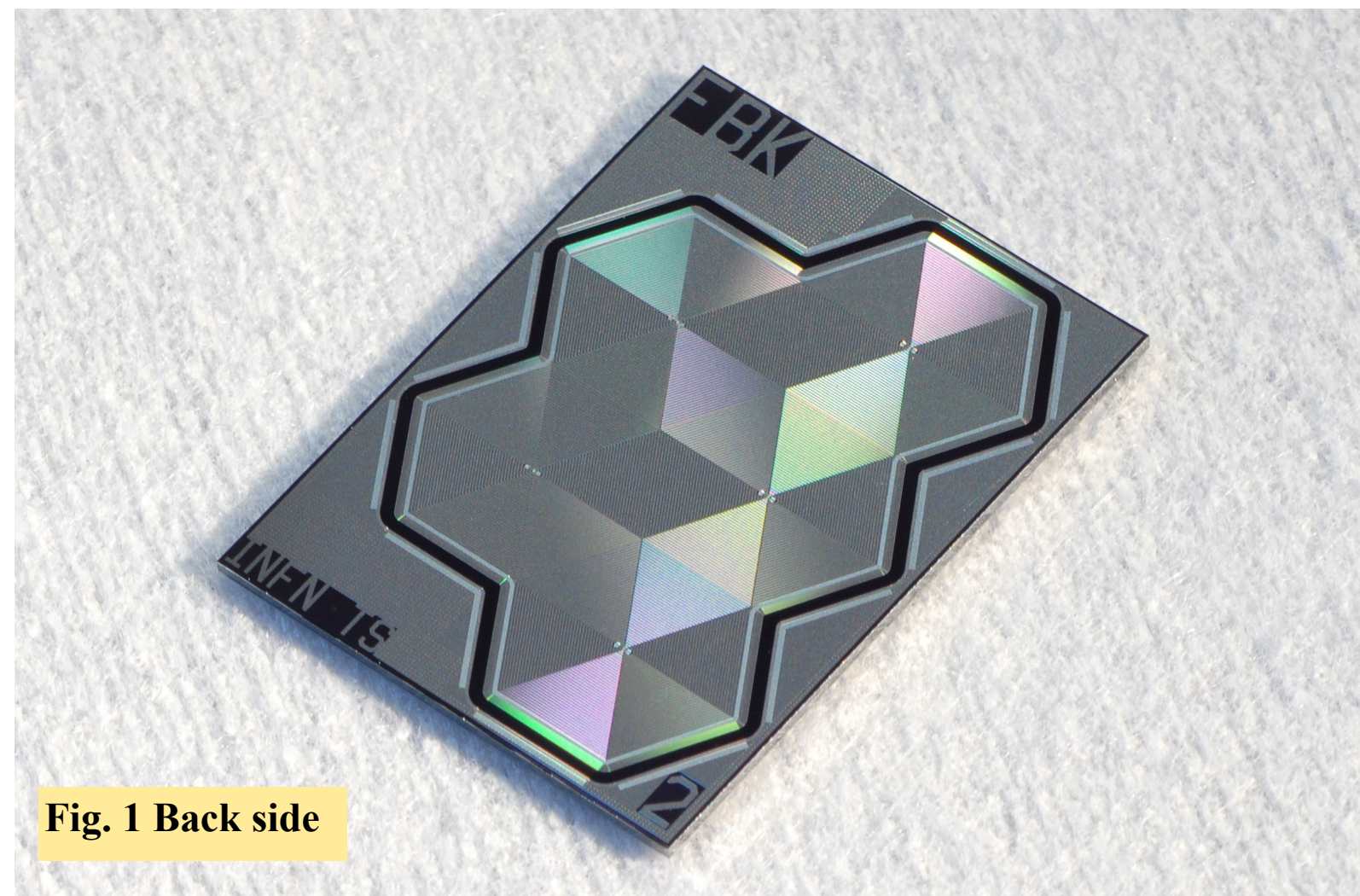


Fig. 1 Back side

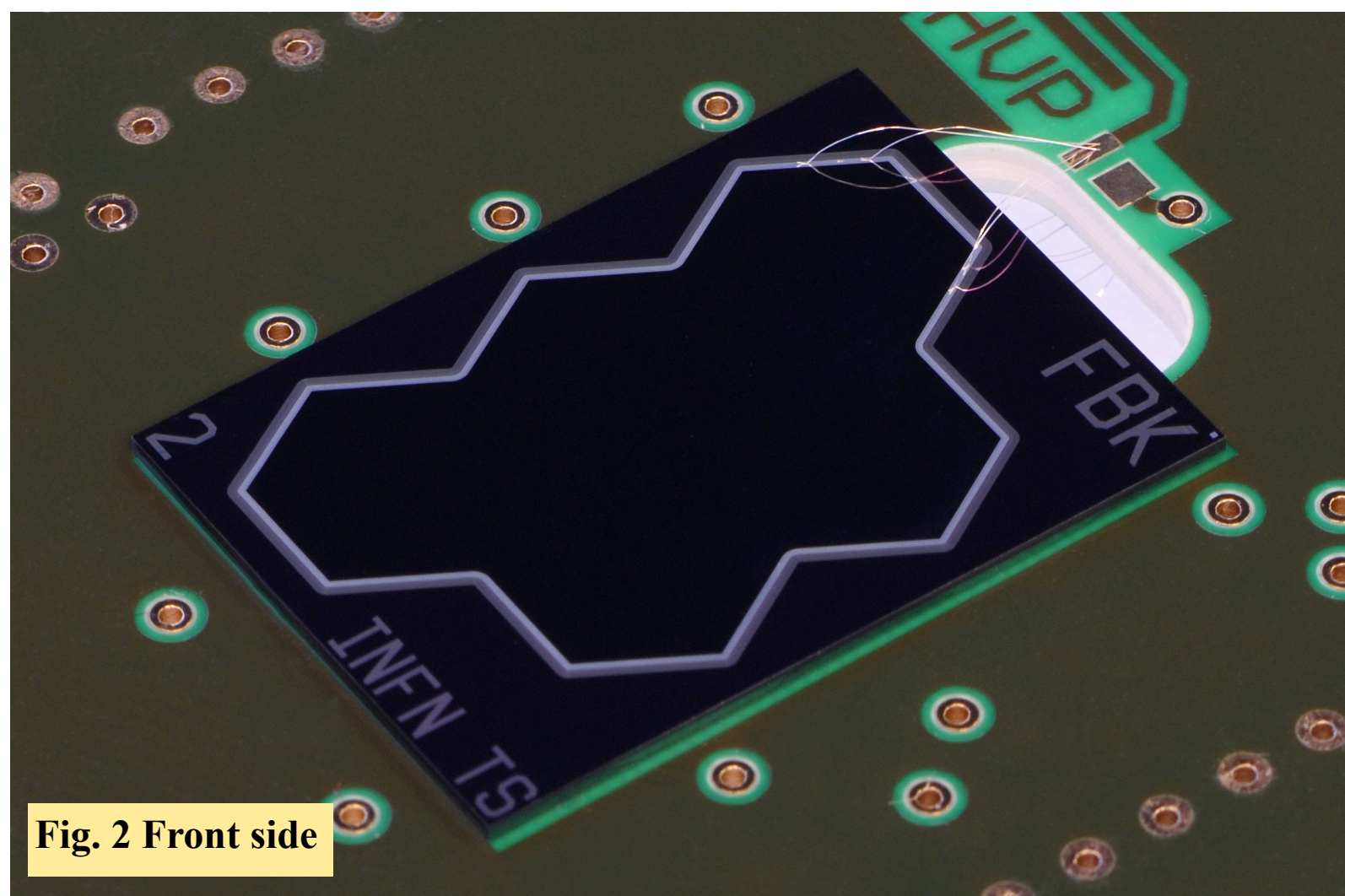


Fig. 2 Front side

### From a single Silicon Drift Diode to a wafer scale mosaic of SDDs

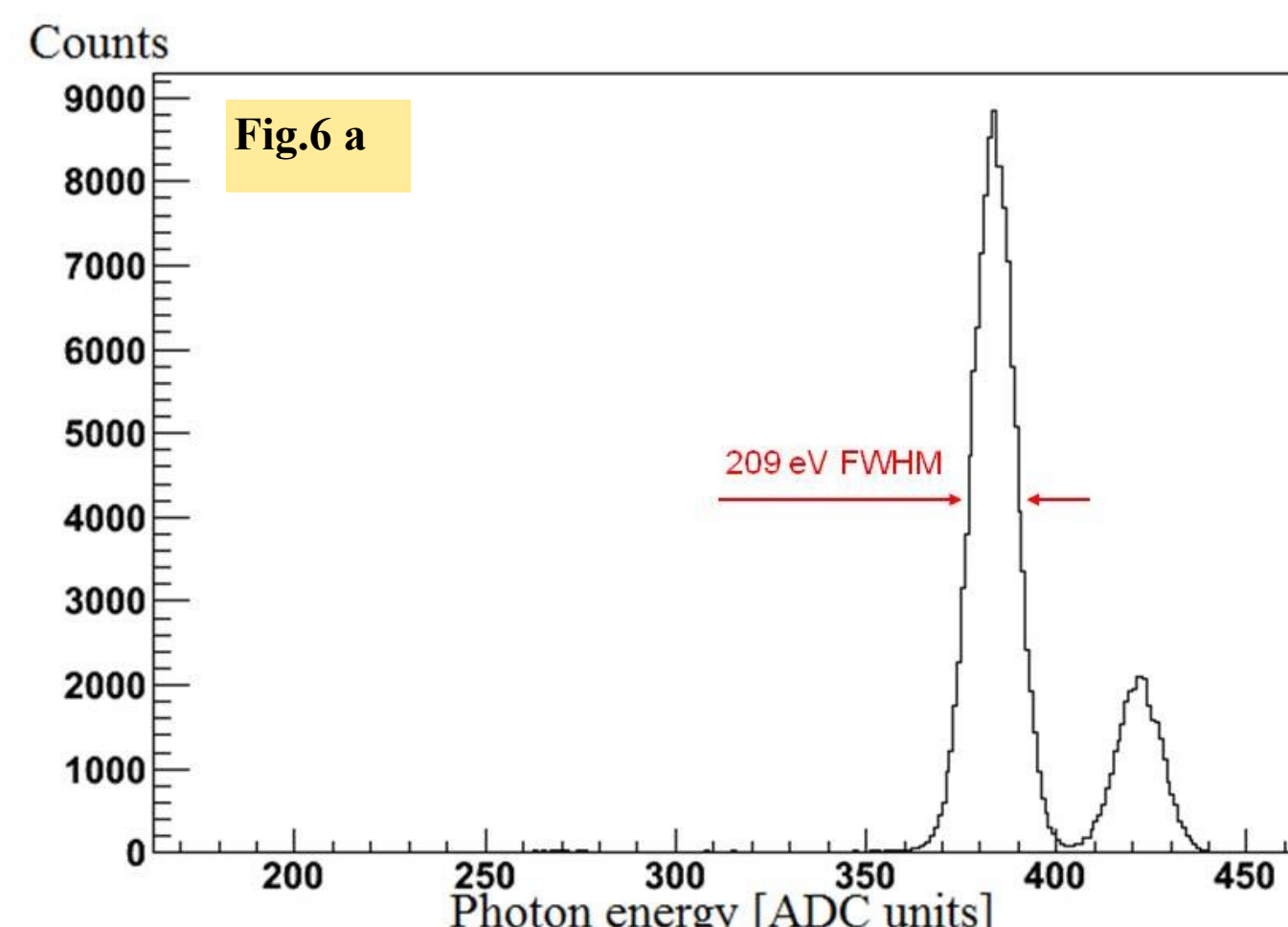
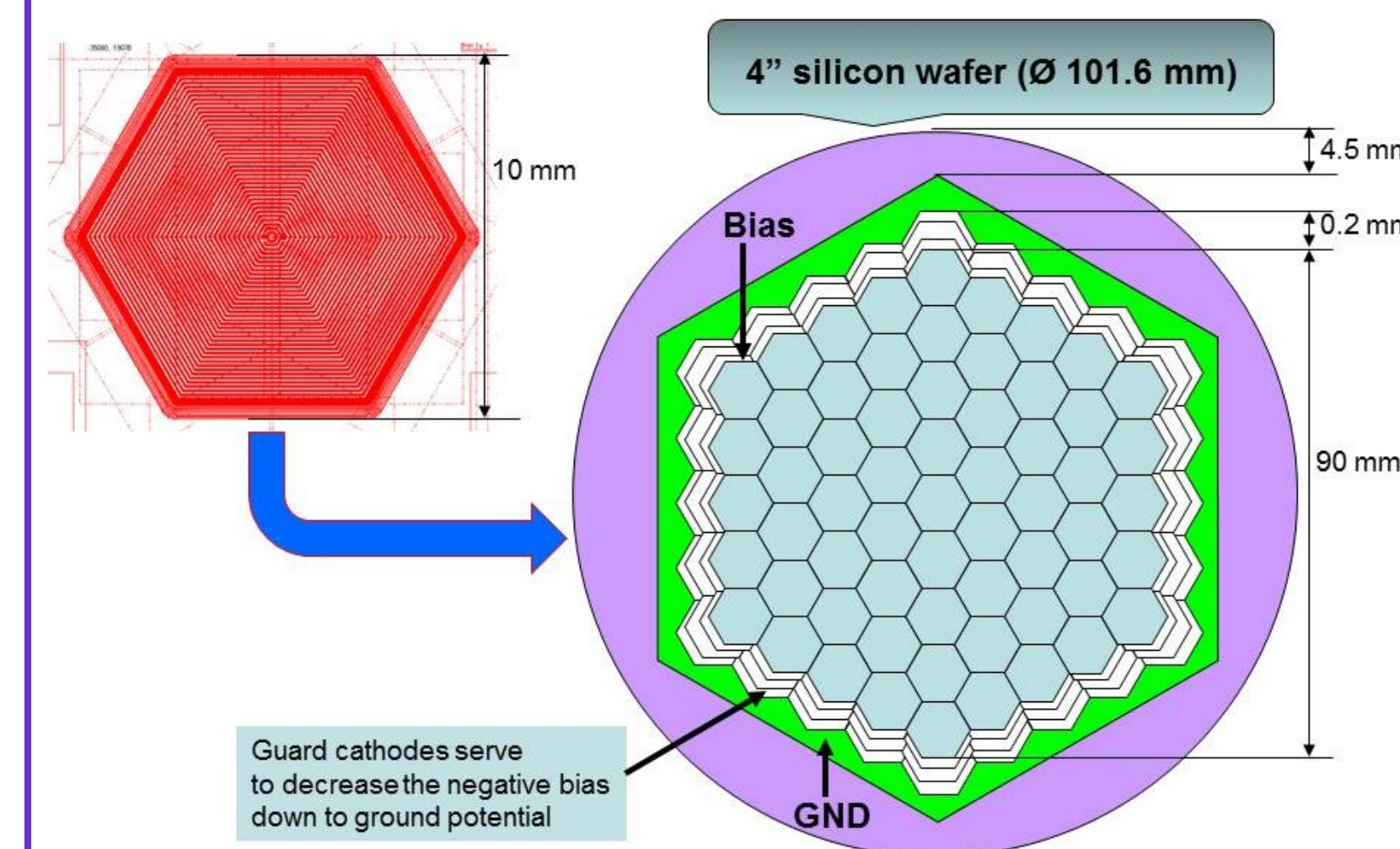


Fig. 6 a

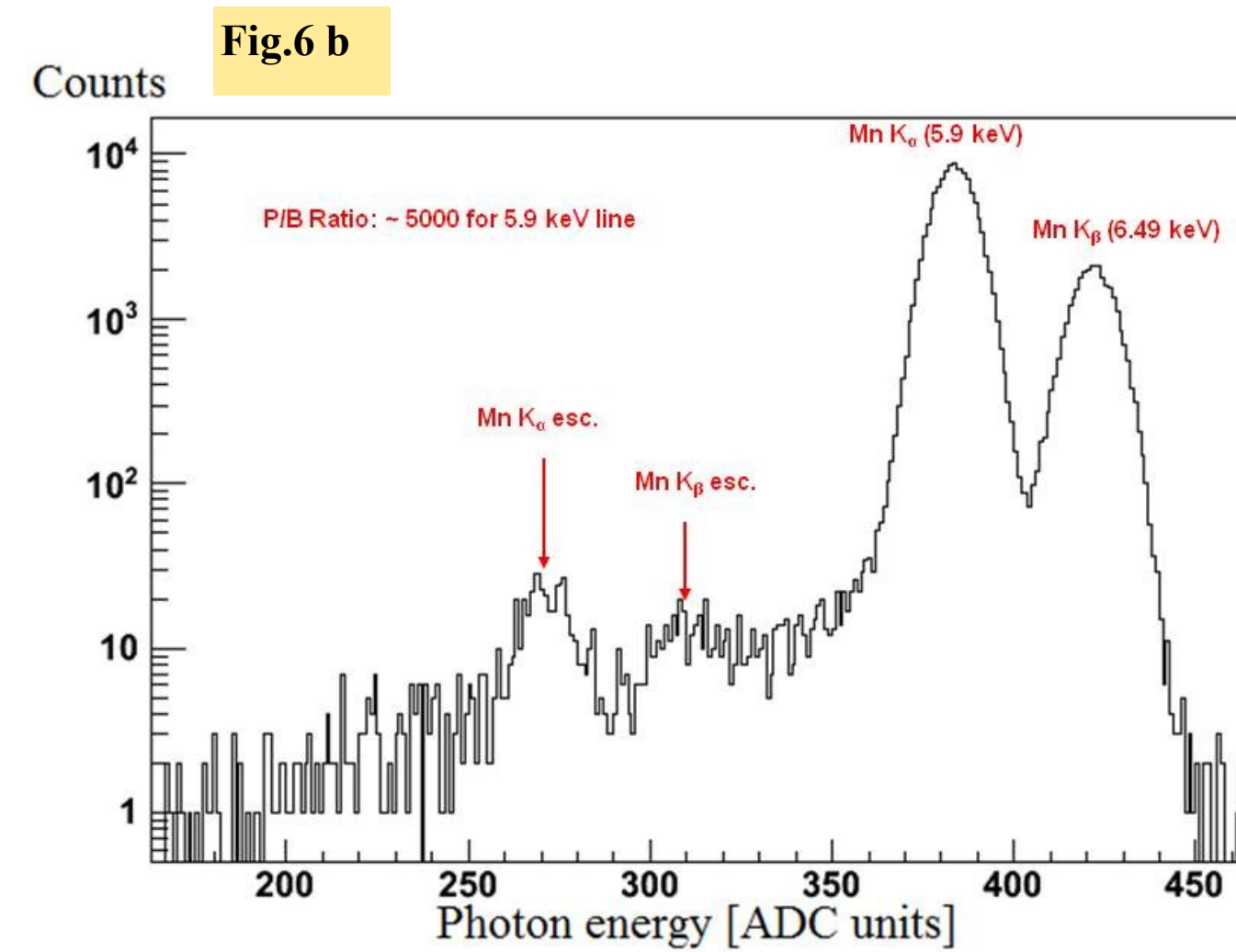


Fig. 6 b

Fig. 6 Linear (a) and logarithmic scale (b) view of <sup>55</sup>Fe spectrum measured at -16 °C with a semi-Gaussian shaper time constant t<sub>SH</sub> = 1 μs (rise time t<sub>R</sub> = 2 μs). The energy resolution for Mn K<sub>α</sub> line is 209 eV FWHM

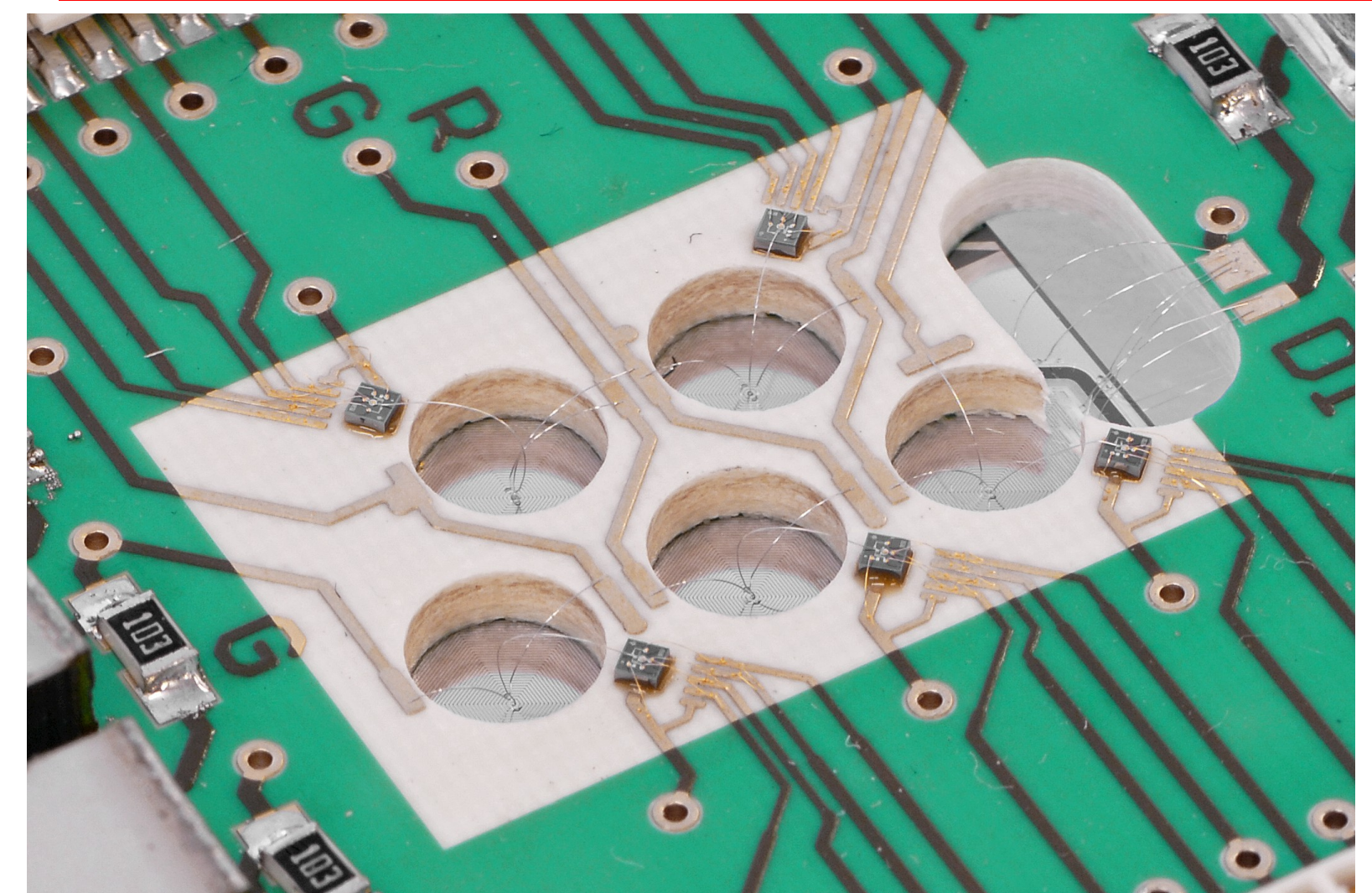


Fig. 4 Mounted detector

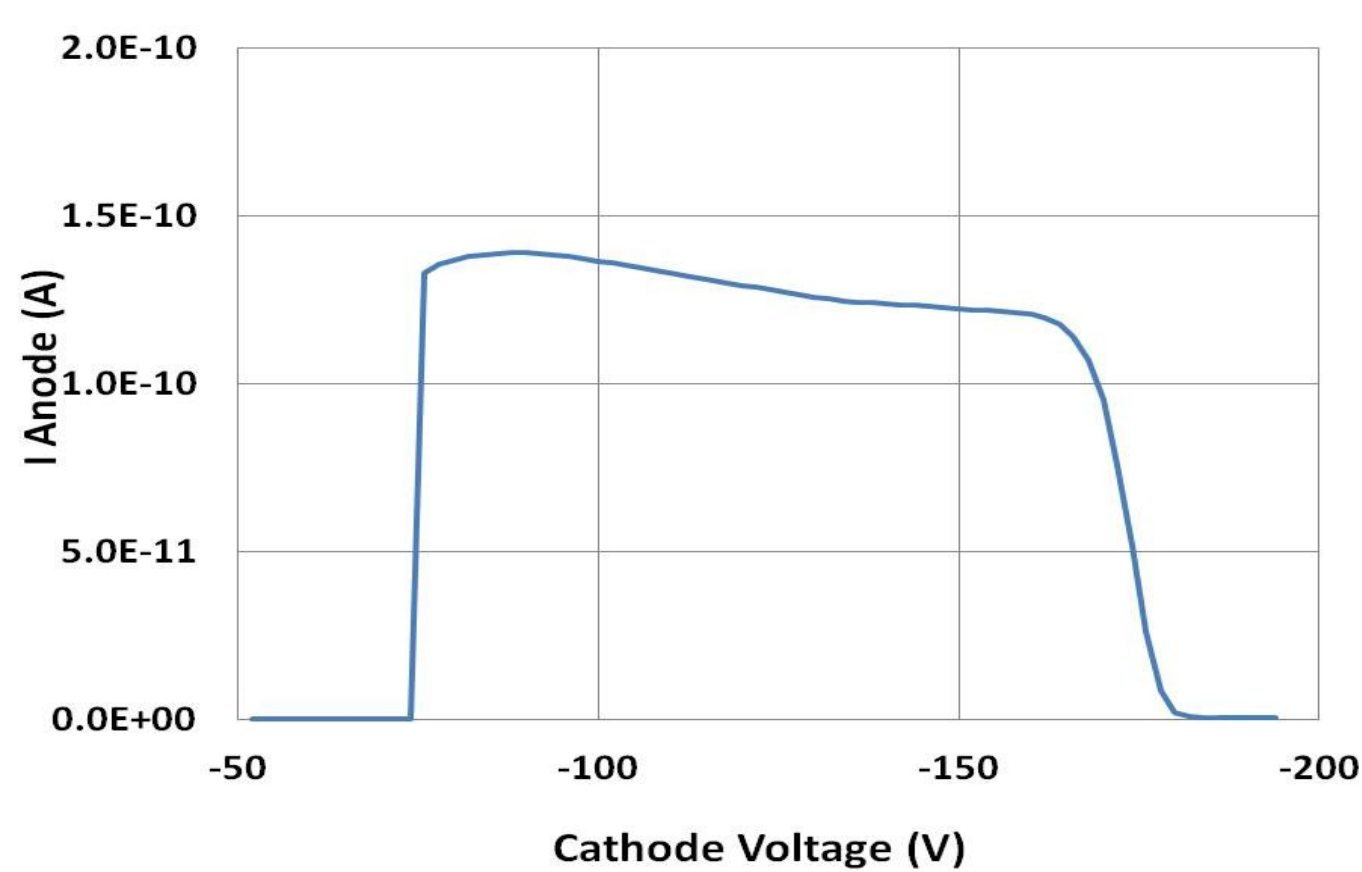


Fig. 3 Readout anode leakage current as a function of the back side bias voltage

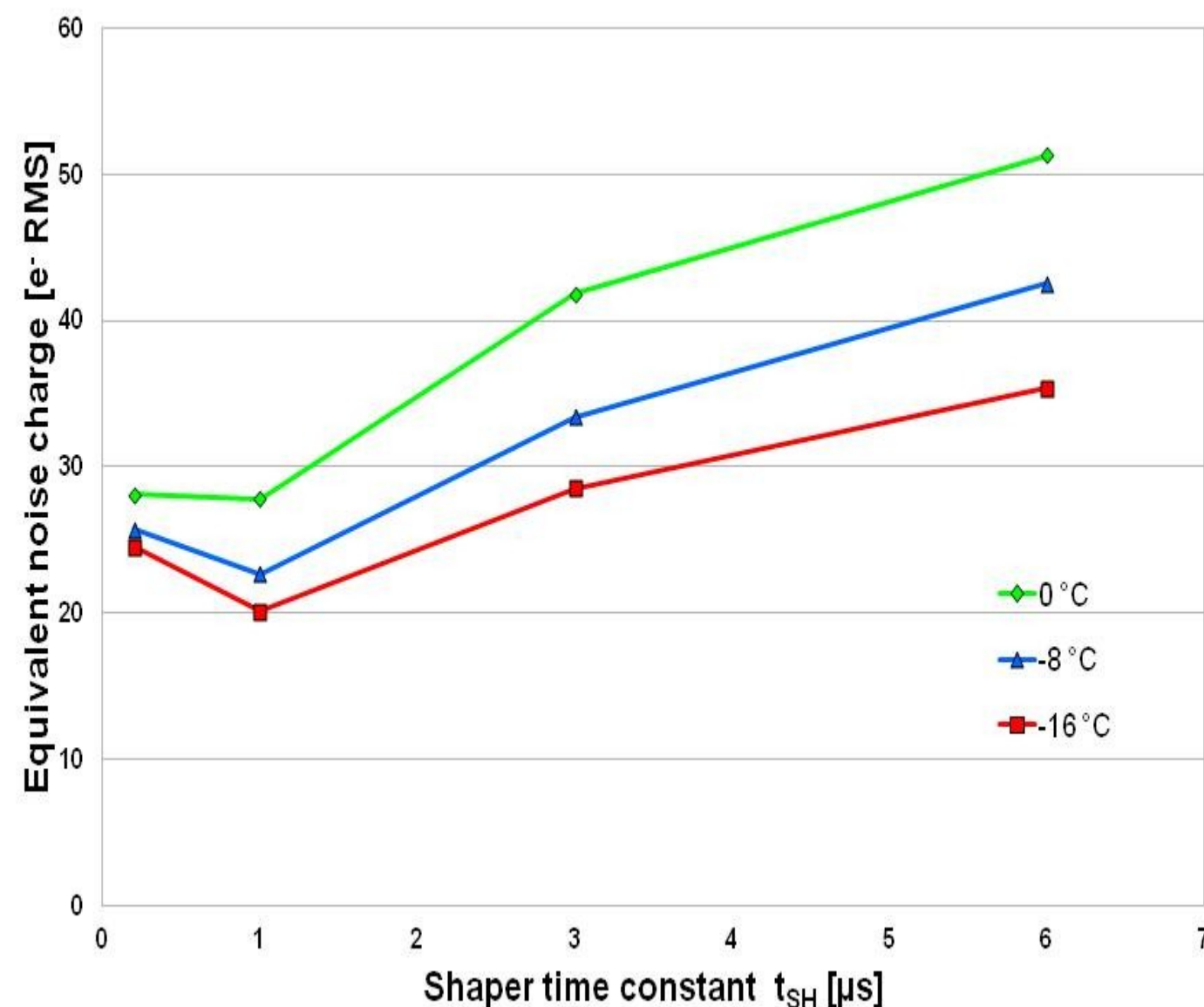


Fig. 5 Equivalent noise charge (e<sup>-</sup> RMS) measured as a function of the shaper time constant t<sub>SH</sub> at three different temperatures: 0 °C; -8 °C; -16 °C

## 3. THE MEASUREMENT SETUP

The spectroscopic performance of the detector was studied at the INFN-Trieste Silicon Detector Laboratory using a <sup>55</sup>Fe radioactive source. The detector under test is mounted on a printed circuit board (Fig. 4) made on high quality dielectric material for radio frequency applications. All bias lines distributed among the five SDDs composing the detector matrix are properly filtered and decoupled to ground close to the detector. Readout anodes of SDDs are connected to corresponding low gate capacitance SF-51 JFETs (C<sub>GS</sub> = 0.4 pF) used as the input transistor of Amptek A250F-NF charge sensitive amplifiers (CSA). The feedback capacitor C<sub>F</sub> = 50 fF and a reset transistor are both integrated on the JFET die, allowing to reduce the stray capacitances at the input for a better noise performance. JFETs and CSAs are both powered by means of batteries in order to minimize the non fundamental noise. The outputs of the CSAs are connected to a Spectroscopy Amplifier which has an internal adjustable shaper, and a 12 bit Peak Sensing ADC, while an oscilloscope is used to measure the leakage current at the anodes by means of the slope of the CSA output voltage. Further details of the readout electronics chain can be found in [7]. Detector and frontend electronics are placed inside a climatic chamber (temperature range of -70 °C ÷ 180 °C) which shields them from external irradiated noise.

## 4. EXPERIMENTAL RESULTS

To analyze the energy resolution of the detector we performed the measurement at three different temperatures (0 °C; -8 °C; -16 °C) using a <sup>55</sup>Fe non-collimated calibration source. A scan of the shaping time constant t<sub>SH</sub> was done at each temperature. Since the shaper is a second order semi-Gaussian filter, the shaped signal rise time t<sub>R</sub> is two times t<sub>SH</sub>, i. e. 0.4, 2, 6 and 12 μs. The equivalent noise charge (ENC) was determined from the pedestal distribution whose energy scale is calibrated by fitting the measured spectra with two Gaussian functions (one for each peak). The results are summarized in Figure 5. Within the used ranges of temperature and shaping time constant, the best resolution of 209 eV FWHM (Fig. 6 a,b) for Mn K<sub>α</sub> line was obtained at -16 °C and t<sub>SH</sub> = 1 μs. The corresponding leakage current was 12 pA. Silicon escape peaks from Mn K<sub>α</sub> and Mn K<sub>β</sub> lines are easily noted on the logarithmic scale (Fig. 6 b). The ratio between Mn K<sub>α</sub> line and the background shelf is about 5000. We expect to improve the spectroscopic performance of the reported device optimizing the frontend electronics, thus reducing the series noise component. For what regards reducing the parallel noise component, the detector needs to be operated at lower temperatures. For the future prototypes, we will introduce technological solutions to decrease the room temperature leakage current.

## REFERENCES

- [1] E. Gatti and P. Rehak, Nucl. Instr. And Meth. A 225 (1984) 608
- [2] C. Fiorini, et al., Nucl. Instr. And Meth. A 568 (2006) 96
- [3] G. De Geronimo, et al., IEEE Trans. Nucl. Sci. 55 (2008) 1604
- [4] P. Rehak, et al., Nucl. Instr. And Meth. A 624 (2010) 260
- [5] D. M. Schlosser, et al., Nucl. Instr. And Meth. A 624 (2010) 270
- [6] M. Feroci, et al., Proc. Of SPIE vol. 7732 (2010) 77321V-1
- [7] G. Zampa, et al., Nucl. Instr. And Meth. A 633 (2011) 15